

## **Bainite formation kinetics in steels and the dynamic nature of the autocatalytic nucleation process**

Ravi, Ashwath M.; Sietsma, Jilt; Santofimia Navarro, Maria

**DOI**

[10.1016/j.scriptamat.2017.06.051](https://doi.org/10.1016/j.scriptamat.2017.06.051)

**Publication date**

2017

**Document Version**

Final published version

**Published in**

Scripta Materialia

**Citation (APA)**

Ravi, A. M., Sietsma, J., & Santofimia Navarro, M. (2017). Bainite formation kinetics in steels and the dynamic nature of the autocatalytic nucleation process. *Scripta Materialia*, 140, 82-86.  
<https://doi.org/10.1016/j.scriptamat.2017.06.051>

**Important note**

To cite this publication, please use the final published version (if applicable).  
Please check the document version above.

**Copyright**

Other than for strictly personal use, it is not permitted to download, forward or distribute the text or part of it, without the consent of the author(s) and/or copyright holder(s), unless the work is under an open content license such as Creative Commons.

**Takedown policy**

Please contact us and provide details if you believe this document breaches copyrights.  
We will remove access to the work immediately and investigate your claim.



## Regular article

# Bainite formation kinetics in steels and the dynamic nature of the autocatalytic nucleation process



Ashwath M. Ravi\*, Jilt Sietsma, Maria J. Santofimia

Dept. of Materials Science and Engineering, Delft University of Technology, Mekelweg 2, Delft 2628 CD, The Netherlands

## ARTICLE INFO

## Article history:

Received 27 February 2017

Received in revised form 2 June 2017

Accepted 29 June 2017

Available online xxx

## Keywords:

Bainite

Kinetics

Nucleation

Isothermal heat treatments

## ABSTRACT

Over the years, a quantitative theory to explain bainite formation kinetics has been proposed based on the nucleation kinetics of bainitic sub-units. Although the theory shows acceptable correlation with experimental results, it is observed that the kinetic models show a certain degree of discrepancy with actual kinetics. It is identified that these mainly arise due to the inadequate estimation of autocatalytic nucleation, especially as a function of progress of bainite formation. With the help of this observation, the kinetic model is modified and a better insight into the process of autocatalytic nucleation, essential in bainite formation, is obtained.

© 2017 Acta Materialia Inc. Published by Elsevier Ltd. This is an open access article under the CC BY-NC-ND license (<http://creativecommons.org/licenses/by-nc-nd/4.0/>).

Among the wide variety of products formed by the decomposition of austenite in steels, formation of bainite is one of the least understood phenomena [1–8]. According to the displacive theory of bainite formation, the rate of bainite formation,  $df/dt$ , is proposed as

$$df/dt = (1 - f)(1 + \lambda f)\kappa_f \quad (1)$$

where  $f$  is the bainite fraction,  $\lambda$  is the autocatalytic parameter and  $\kappa_f$  is the rate parameter which accounts for the thermally activated nature of the bainite nucleation process [9–15]. This equation was derived based on the displacive mechanism of bainite formation [9,13]. Bainite formation in steels begins with nucleation of bainitic ferrite at austenite grain boundaries. Subsequently, nucleation continues further through autocatalytic nucleation of bainitic ferrite at the newly created bainitic ferrite/austenite interfaces [16]. The difference in nucleation rate of bainite formed by autocatalysis compared to the nucleation rate of bainite due to grain-boundary nucleation is accounted for by the term  $\lambda f$  in Eq. (1) [9–13]. Most studies applying Eq. (1) treat  $\lambda$  as an empirical dimensionless fitting constant [13]. The values obtained for  $\lambda$  are however not satisfactorily analysed in the literature [6]. Recently, the present authors [15] proposed that  $\lambda$  is determined by the difference in activation energy for bainite nucleation at austenite grain boundaries and bainite

nucleation at bainite/austenite interfaces (autocatalytic nucleation) and can be expressed as

$$\lambda = \exp\left(\frac{\Delta Q^*}{kT}\right) \quad (2)$$

where  $\Delta Q^*$  is the difference ( $Q_G^* - Q_A^*$ ) in the activation energy for grain-boundary nucleation ( $Q_G^*$ ) and autocatalytic nucleation ( $Q_A^*$ ),  $k$  is Boltzmann's constant and  $T$  is the bainite formation temperature.

Studies claim that nucleation based models using the functional form described in Eq. (1) accurately predict the bainite formation kinetics in steels [9,11–13,15]. However, a close examination of the published results suggests that these models still show a certain degree of miscalculation of kinetics [10–12,14]. Santofimia et al. [13] evaluated the applicability of several kinetic models which are based on the displacive theory of bainite formation. They also observed that the models imprecisely estimate the nucleation rate and called for a better treatment of autocatalytic nucleation [13]. Although these discrepancies are rarely investigated in detail, they have been attributed to improper estimation of final volume fraction of bainite or to unaccounted carbide precipitation [13]. This implies that these discrepancies are generally considered to be due to the improper estimation of the degree of carbon enrichment of austenite, since the carbon content in austenite determines final volume fraction of bainite [10,14] and the degree of carbide precipitation during bainite formation [11].

In the current work, it is shown that an adequate estimation of carbon enrichment alone is not sufficient to accurately simulate the

\* Corresponding author.

E-mail addresses: [A.M.Ravi@tudelft.nl](mailto:A.M.Ravi@tudelft.nl) (A.M. Ravi), [J.Sietsma@tudelft.nl](mailto:J.Sietsma@tudelft.nl) (J. Sietsma), [M.J.SantofimiaNavarro@tudelft.nl](mailto:M.J.SantofimiaNavarro@tudelft.nl) (M.J. Santofimia).

**Table 1**  
Chemical compositions of steels used for study (values in wt%).

Steel	C	Mn	Si	Mo	Al	Reference
S1	0.2	3	–	–	–	Current work
S2	0.2	3.51	1.52	0.25	0.04	[17]

rate of bainite formation. A strong argument for this is presented here. A fundamental change in the assumptions for autocatalytic nucleation, especially as a function of increasing bainite fraction, is required to adequately estimate bainite formation kinetics. Based on these new assumptions, the bainite kinetics is simulated and compared with experimental results.

The compositions of the steels used for the present work are given in Table 1. Studies in the current work have been carried out using kinetic data obtained from isothermal bainite formation experiments on Steel S1. The bainite formation experiments were carried out in a Bähr DIL805A/D dilatometer. Specimens were first austenized at 1273 K and then isothermally held at 653 K. The bainite fraction formed as a function of time was determined based on the dilatometer data obtained. Results obtained from these studies were further validated using the kinetic data published in the literature on Steel S2 (isothermal treatment at 603 K for 1 h after austenization at 1173 K) [17].

Fig. 1 (a) gives the experimentally obtained bainite fraction,  $f$  vs time for both steels, while Fig. 1 (b) gives the rate of bainite formation,  $df/dt$ , as bainite formation progresses. Fig. 1 (c) and (d) shows experimentally obtained  $(df/dt)_v$  as a function of  $f$  in Steel S1 and Steel S2 respectively, where  $(df/dt)_v$  is the rate of bainite formation per unit volume of untransformed austenite (volume fraction available for bainite formation). It is given as

$$(df/dt)_v = (df/dt)/(1-f). \quad (3)$$

$(df/dt)_v$  is an important parameter in understanding the bainite formation kinetics. The overall rate of bainite nucleation in steels mainly depends number of grain-boundary nucleation sites available and the potency of these nucleation sites to form bainitic ferrite sub-units. It should be noted that the rate of autocatalytic nucleation also depends on the rate at which grain-boundary nucleation occurs, since grain-boundary nucleation is a prerequisite for creating bainite/austenite interfaces and subsequent autocatalytic nucleation. The potency of grain-boundary nucleation sites to transform into bainitic sub-units and facilitate autocatalytic nucleation is influenced by rate governing parameters such as bainite formation temperature and carbon concentration in austenite [12,13,18,19].  $(df/dt)_v$  gives a measure of this potency. Physically, it represents the rate at

which grain-boundary nucleation sites can contribute to the overall nucleation rate. Numerically,  $(df/dt)_v$  can be determined using experimentally obtained  $(df/dt)$  data and the corresponding bainite fraction,  $f$ .

The displacive theory of bainite formation suggests that the rate of bainite formation is determined by the nucleation of bainitic sub-units. Thus from Fig. 1 (c) and (d), the rate at which bainite nucleation occurs within the available austenite can be interpreted. It can be seen from these figures that the rate of austenite transformation into bainite constantly changes as bainite formation progresses.

One of the well documented reasons for such a change in the austenite transformation rate is due to the possible carbon enrichment of austenite during bainite formation [20]. Since  $(df/dt)_v$  is a measure of the rate of austenite to bainite transformation, the effect of carbon enrichment on the rate of bainite formation can be understood by interpreting its effect on  $(df/dt)_v$ . Using Eqs. (1) and (3),  $(df/dt)_v$  can be given as

$$(df/dt)_v = (1 + \lambda f)\kappa_f. \quad (4)$$

With the help of Eq. (4) and the kinetic model proposed by the authors [15], a physically based interpretation of  $(df/dt)_v$  can be derived since the carbon enrichment of residual austenite during bainite formation is well accounted for in the proposed model. The underlying principles used in Ref. [15] for calculation of bainite formation kinetics are similar to other published models [12,13,18,19] that use displacive theory of bainite formation. In Ref. [15], the effect of carbon enrichment on the rate of bainite formation is calculated using a fitting constant,  $X_b$ .  $X_b$  accounts for the carbon which does not participate in the carbon enrichment of austenite. Using the approach given in Ref. [15],  $\kappa_f$  in Eq. (1) can be given as

$$\kappa_f \propto (T_h - T)(T'_0 - T) \exp\left(-\frac{Q_G^*}{kT}\right) \quad (5)$$

where  $T_h$  and  $T'_0$  are the critical temperatures which define the thermodynamic conditions for bainite formation [3]. The factor  $(T_h - T)$  signifies the driving force available for bainite nucleation, while the factor  $(T'_0 - T)$  signifies the driving force available for bainite growth [3].  $T_h$ ,  $T'_0$  and  $Q_G^*$  are all functions of carbon concentration of austenite [3,15,20] and can be expressed in terms of  $f$  and  $X_b$  [15]. Studies suggest that  $T_h$  and  $T'_0$  decrease linearly and  $Q_G^*$  increases linearly with increasing carbon enrichment of austenite [15].

In order to understand the effect of carbon enrichment of austenite on the rate of bainite formation,  $(df/dt)_v$  was calculated assuming varying degrees of the carbon enrichment (by numerically varying the value of  $X_b$ ) using Eqs. (2), (4), and (5). In Eq. (5), the proportionality constant is a material dependent parameter and is calculated according to Ref. [15] (for Steel S1 =  $1.92 \text{ s}^{-1} \text{ K}^{-2}$ ). According to the

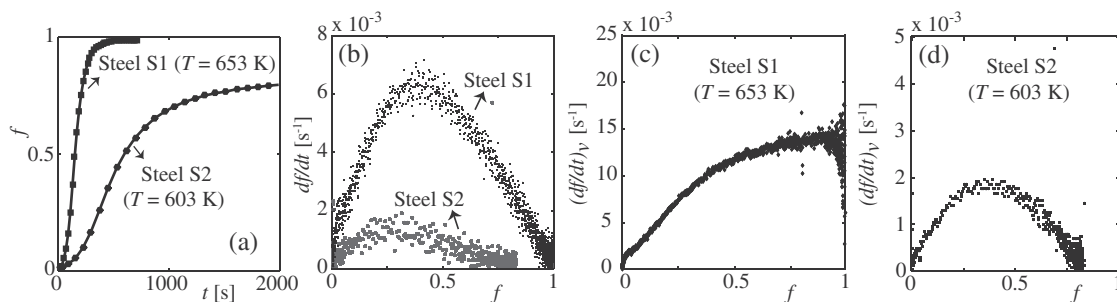


**Fig. 1.** (a) Comparison of experimentally obtained kinetics (Steel S1 at  $T = 653 \text{ K}$ , Steel S2 at  $T = 603 \text{ K}$ ). (b) Experimentally obtained  $df/dt$  vs  $f$ , (c, d) Experimentally obtained  $(df/dt)_v$  vs  $f$ .

definition of  $X_b$  [15], the degree of carbon enrichment of austenite increases for decreasing values of  $X_b$  (Fig. 2 (a)). The varying trends of  $(df/dt)_v$  as a function of  $X_b$  shed light on the effect of the carbon enrichment of austenite on bainite formation kinetics.  $(df/dt)_v$  can be calculated for various  $X_b$  values assuming the initial  $Q_G^*$  value (at  $f=0$ , referred as  $Q_{GX}^*$ ) to be 155 kJ/mol and  $\Delta Q^*$  to be 20 kJ/mol. These assumed values are based on previously published data for the activation energy for bainite nucleation [11,12,15,21] in the literature.

Fig. 2 (a) shows the  $(df/dt)_v$  trends as a function of bainite fraction by assuming four different  $X_b$  values in Steel S1 for isothermal bainite formation at 653 K. The assumed  $X_b$  values can be related to the overall carbon concentration of the steel,  $\bar{X}$ . For instance, in Fig. 2 (a),  $X_b = 0.8\bar{X}$  suggests that  $X_b$  is assumed to be equal to 80% of the overall carbon concentration of steel. In Fig. 2 (a), a maximum is seen to occur for  $X_b < \bar{X}$ . Furthermore, the bainite fraction at which the maximum occurs shifts to a lower value when the degree of carbon enrichment of austenite is higher (i.e., when  $X_b$  is lower). It must be noted that although  $(df/dt)_v$  is only shown for Steel S1, similar trends apply for Steel S2 (or any other steel composition) since Eqs. (2), (4), and (5) are applicable for all steels.

Fig. 2 (a) can be compared with the experimental  $(df/dt)_v$  curves in Fig. 1 (c) and (d) in order to understand the effect of carbon enrichment of austenite on bainite kinetics. It can be seen that the carbon enrichment of austenite during bainite formation in Steel S2 is much greater than for Steel S1 in agreement with Fig. 2 (a); a clear maximum is visible in Fig. 1 (d) at a low value for bainite fraction ( $f \approx 0.4$ ) while the maximum in Fig. 1 (c) appears close to the end of the bainite formation process ( $f \approx 0.9$ ) and is less pronounced. This can be attributed to the chemical composition of the steels. Steel S1 is a silicon-free steel and exhibits carbide precipitation during bainite formation, while in Steel S2, carbide precipitation is suppressed, leading to greater carbon enrichment of austenite [17].

The carbon enrichment of austenite (whose degree increases as bainite fraction increases) should ideally lead to a decrease in rate of bainite formation as bainite fraction increases. Nevertheless, Fig. 2 (a) shows an increase in rate of bainite formation until a maximum is reached at a relatively high bainite fraction. This is due to the competition between increasing autocatalytic nucleation and increasing degree of carbon enrichment as bainite fraction increases. The carbon enrichment of austenite affects both autocatalytic and grain-boundary nucleation. As the bainite formation progresses, both the activation energy for autocatalytic nucleation and the activation energy for grain-boundary nucleation decrease with increasing degree of carbon enrichment. On the other hand, the rate of autocatalytic nucleation increases initially as the bainite formation progresses as a result of increased number density of autocatalytic nucleation sites due to increasing bainite fraction. When

a certain bainite fraction is formed, the carbon enrichment of the austenite becomes too high to sustain an increasing rate of bainite formation. This results in the maximum seen in Fig. 2 (a). This explanation of the maximum is consistent with the observation that for  $X_b = \bar{X}$ , which implies that carbon enrichment of austenite does not take place, no maximum occurs. Based on these trends, it can be concluded that the maximum is due to carbon enrichment of austenite during bainite formation.

However, by further comparing Fig. 2 (a) to Fig. 1 (c) and (d), it can be seen that the carbon enrichment alone is insufficient to accurately simulate the experimentally obtained trends. The non-linear increase in rate of bainite formation before the maximum (clearly seen in Fig. 1 (c)) is not predicted by the current description (Fig. 2 (a)). This calls for revisiting the assumptions used for simulating bainite formation kinetics.

As mentioned previously, most studies use a constant  $\lambda$  to account for autocatalytic nucleation during bainite formation. As given in Eq. (2),  $\lambda$  is dependent on the difference in the activation energy for grain-boundary bainite nucleation and autocatalytic bainite nucleation. This difference is assumed to be constant [15]. This suggests that the activation energy for grain-boundary nucleation and autocatalytic nucleation increase at the same rate with increasing  $f$ .

However, it can be argued that  $\lambda$  will not remain constant throughout the bainite formation process. Bainite nucleation is an interfacial process and thus depends on the chemistry and the morphological characteristics of the interface at which bainite nucleates. These aspects heavily depend on the type of the interface [22,23]. This suggests that the activation energy required for grain boundary nucleation can be expected to be different compared to the activation energy required for autocatalytic nucleation. Furthermore, bainitic growth is a displacive process and leads to plastic deformation of surrounding austenite matrix [2,16,24]. This suggests that the dislocation densities around the bainite/austenite interfaces may vary as the bainitic growth continues to form sheaves. Therefore, the activation energies of autocatalytic nucleation and of grain-boundary nucleation will increase at different rates. To account for these effects, it is assumed that the difference in the activation energy is a function of bainite fraction  $f$  can be expressed as,

$$\Delta Q^* = Q_G^* - Q_A^* = \Delta Q_X^* + \theta f \quad (6)$$

where  $\theta$  is the proportionality constant between  $\Delta Q^*$  and  $f$ .  $\Delta Q_X^*$  is  $\Delta Q^*$  at  $f=0$ .

Using the above assumption of  $\Delta Q^*$  being linearly related to  $f$ , the trends for  $(df/dt)_v$  were recalculated for various  $\theta$  values in Steel S1 for isothermal bainite formation at 673 K (Fig. 2 (b)), using the same values as for Fig. 2 (a). It must be noted that for Fig. 2 (a),  $\Delta Q^*$  was assumed to be constant. For Fig. 2 (b),  $\Delta Q^*$  is assumed to depend on  $f$ , according to Eq. (6), and  $\Delta Q_X^*$  is assumed to be constant. Furthermore, in the calculations, in order to account for the effect of a slight carbon enrichment,  $X_b$  is considered to be equal to  $0.99\bar{X}$ .

It can be seen in Fig. 2 (b) that the calculated trends are now much closer to the experimentally obtained  $(df/dt)_v$  curve in Fig. 1 (c). The non-linear increase in rate of bainite formation before the maximum is predicted by the calculated trends. Based on these results, it can be said that a combination of  $X_b$  and  $\theta$  values is required to simulate the experimental trends observed. With the help of these results, the kinetic model proposed in Ref. [15] was modified and  $\theta$  was introduced as a new fitting parameter. The calculated kinetics from the model was compared with kinetics data obtained by dilatometry experiments in the current work as well as with published kinetic data in the literature [17].

Fig. 3 (a), (b) shows the comparison between simulated and experimentally derived  $(df/dt)_v$  as a function of bainite fraction. It

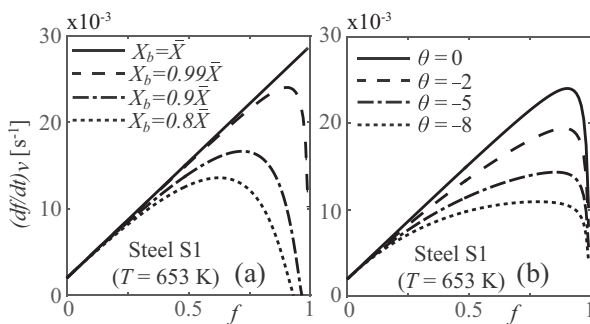
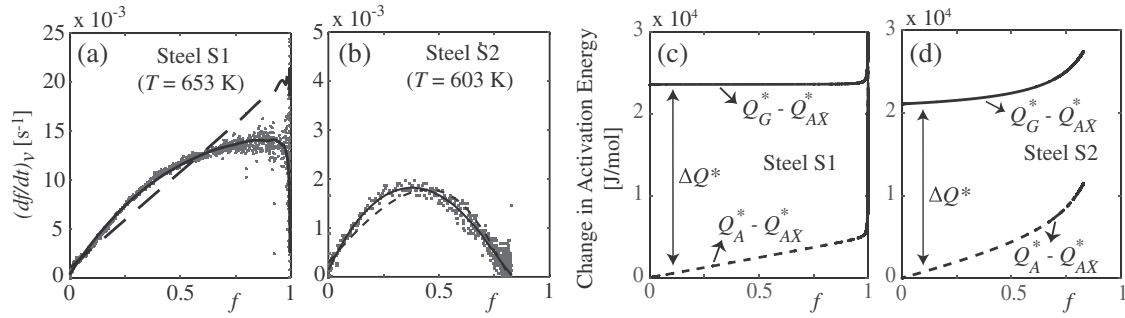


Fig. 2. Calculated  $(df/dt)_v$  vs  $f$  in Steel S1 (Bainite formation temperature = 653 K) for (a) varying degrees of carbon enrichment (varying  $X_b$ ) and (b) for varying  $\theta$  values (in kJ/mol), with  $X_b = 0.99\bar{X}$ .



**Fig. 3.** (a, b) Experimental (markers) and calculated (lines)  $(df/dt)_v$  vs  $f$  (dashed line:  $\theta = 0$  kJ/mol, solid line:  $\theta = -4.8$  kJ/mol (Steel S1) and  $-6.1$  kJ/mol (Steel S2)). (c, d) Change in activation energy for nucleation (dashed line: autocatalytic nucleation, solid line: grain-boundary nucleation). The bainite formation temperature for Steel S1 is 653 K and Steel S2 is 603 K respectively.  $Q_{AX}^*$  is the initial  $Q_A^*$  at  $f = 0$ .

can be observed that  $(df/dt)_v$  is accurately calculated with the modified model. This suggests that the nucleation rate and consequently, the activation energy for bainite nucleation is calculated precisely.

The values for the fitting parameters obtained are given in Table 2. It is observed that the  $\theta$  parameter shows a negative value. This suggests that the activation energy for autocatalytic nucleation increases faster than the activation energy for grain-boundary nucleation as a function of bainite fraction, as seen in Fig. 3 (c) and (d). These figures give the change of activation energy for bainite nucleation as a function of  $f$  for both autocatalytic and grain-boundary nucleation. The change in activation energy is calculated with respect to the initial activation energy for autocatalytic nucleation,  $Q_{AX}^*$  (i.e.  $Q_A^*$  at  $f = 0$ ). These figures also show that the activation energy for grain-boundary nucleation in Steel S1 only increases significantly as bainite fraction approaches unity. This is due to the limited carbon enrichment in Steel S1 ( $X_b = 0.99\bar{X}$ ).

In a physical sense, the rate at which bainite formation progresses can be estimated by calculating activation energies for both grain-boundary nucleation and autocatalytic nucleation. As discussed in already published literature, carbon enrichment of austenite leads to increase in the activation energy for bainite nucleation, which leads to a decreasing rate of bainite formation as the bainite fraction increases. However, the rate at which the activation energies for grain-boundary nucleation and for autocatalytic nucleation increase is different. This suggests that the impact of carbon enrichment on autocatalytic nucleation and grain-boundary nucleation might be different. Also, other factors can lead to an increase in the activation energy for bainite formation, since the ability of austenite to transform into bainite is not just affected by its carbon enrichment during bainite formation. One other factor can be the plastic deformation of austenite, that is associated with bainite formation [1,2,25]. These factors are accounted for by the parameter  $\theta$ . Ongoing studies by the present authors on  $\theta$  also show that  $\theta$  can be affected by the grain size of the austenite in which the bainite formation occurs. Such behaviour can be due to the reducing volume of the austenite grains within which bainite formation can occur as the bainite fraction increases and to the stress state associated with this residual austenite volume (due to surrounding bainite). It can be, therefore,

**Table 2**

Values of fitting parameters obtained (95% Confidence Interval provided in parentheses).

Steel	$T$ (K)	$\bar{X}$ (wt%)	$X_b$ (wt%)	$Q_{GX}^*$ (kJ/mol)	$\Delta Q_X^*$ (kJ/mol)	$\theta$ (kJ/mol)
S1	653	0.2	0.199 ( $\pm 0.001$ )	164.5 ( $\pm 0.1$ )	23.6 ( $\pm 0.3$ )	-4.8 ( $\pm 0.2$ )
S2	603	0.2	0.1 ( $\pm 0.01$ )	165.2 ( $\pm 0.1$ )	21.0 ( $\pm 0.1$ )	-6.1 ( $\pm 0.1$ )

envisaged that as the bainite formation progresses, the austenite matrix in which the bainite formation occurs undergoes several changes, thereby affecting the bainite formation kinetics.

In summary, even though a kinetic theory for bainite formation based on the displacive mechanism of bainite growth has been well established, literature evidence calls for a more detailed treatment since deviations larger than the experimental uncertainty are found. The reasons behind such discrepancies are investigated in detail in the current work. The proposed kinetic theory suggests that carbon enrichment of the austenite during bainite formation has a different influence on the activation energies for grain-boundary and autocatalytic nucleation. Furthermore, factors such as the instantaneous deformation state of the austenite and the instantaneous volume of the austenite grain can be expected to affect the bainite kinetics as well. A new fitting parameter,  $\theta$ , is introduced to the kinetic model given in Ref. [15] to account for these factors.  $\theta$  is a physical entity which expresses the difference between the activation energy for autocatalytic bainite nucleation and grain-boundary nucleation as a function of bainite fraction. This interpretation improves the quantitative theory and provides excellent correlation between experimental and calculated bainite kinetics.

The research leading to these results has received funding from the European Research Council under the European Union's Seventh Framework Programme (FP/2007–2013)/ERC Grant Agreement n. [306292].

## References

- [1] L.C.D. Fielding, Mater. Sci. Technol. 29 (2013) 383–399. <http://dx.doi.org/10.1179/1743284712Y.0000000157>.
- [2] H.K.D.H. Bhadeshia, D.V. Edmonds, Acta Metall. 28 (1980) 1265–1273. [http://dx.doi.org/10.1016/0001-6160\(80\)90082-6](http://dx.doi.org/10.1016/0001-6160(80)90082-6).
- [3] H.K.D.H. Bhadeshia, Acta Metall. 29 (1981) 1117–1130. [http://dx.doi.org/10.1016/0001-6160\(81\)90063-8](http://dx.doi.org/10.1016/0001-6160(81)90063-8).
- [4] M. Hillert, ISIJ Int. 35 (1995) 1134–1140. <http://dx.doi.org/10.2355/isijinternational.35.1134>.
- [5] M. Hillert, Metall. Mater. Trans. A 25 (1994) 1957–1966. <http://dx.doi.org/10.1007/BF02649044>.
- [6] H.K.D.H. Bhadeshia, Mater. Sci. Eng. A 273–275 (1999) 58–66. [http://dx.doi.org/10.1016/S0921-5093\(99\)00289-0](http://dx.doi.org/10.1016/S0921-5093(99)00289-0).
- [7] A. Borgenstam, M. Hillert, J. Agren, Acta Mater. 57 (2009) 3242–3252. <http://dx.doi.org/10.1016/j.actamat.2009.03.026>.
- [8] F. Caballero, M. Miller, C. Garcia-Mateo, Acta Mater. 58 (2010) 2338–2343. <http://dx.doi.org/10.1016/j.actamat.2009.12.020>.
- [9] H.K.D.H. Bhadeshia, J. Phys. 43 (1982) 443–448.
- [10] N.A. Chester, H.K.D.H. Bhadeshia, J. Phys. IV France 07 (1997) 41–46. <http://dx.doi.org/10.1051/jp4:1997506>.
- [11] S.M.C. van Bohemen, J. Sietsma, Int. J. Mater. Res. 99 (2008) 739–747. <http://dx.doi.org/10.3139/146.101695>.
- [12] S.M.C. van Bohemen, D.N. Hanlon, Int. J. Mater. Res. 103 (2012) 987–991. <http://dx.doi.org/10.3139/146.110744>.
- [13] M.J. Santofimia, F.G. Caballero, C. Capdevila, C. Garcia-Mateo, C.G. de Andres, Mater. Trans. 47 (2006) 1492–1500. <http://dx.doi.org/10.2320/matertrans.47.1492>.
- [14] G. Sidhu, S. Bhole, D. Chen, E. Essadiqi, Scr. Mater. 64 (2011) 73–76. <http://dx.doi.org/10.1016/j.scriptamat.2010.09.009>.

- [15] A.M. Ravi, J. Sietsma, M.J. Santofimia, *Acta Mater.* 105 (2016) 155–164. <http://dx.doi.org/10.1016/j.actamat.2015.11.044>.
- [16] H.K.D.H. Bhadeshia, *Bainite in Steels: Transformations, Microstructure and Properties*, *Matsci Series IOM Communications*. 2001.
- [17] A. Navarro-López, J. Sietsma, M.J. Santofimia, *Metall. Mater. Trans. A* 47 (2016) 1028–1039. <http://dx.doi.org/10.1007/s11661-015-3285-6>.
- [18] H. Matsuda, H.K.D.H. Bhadeshia, *Proc. R. Soc. Lond. A* 460 (2004) 1707–1722. <http://dx.doi.org/10.1098/rspa.2003.1225>.
- [19] G.I. Rees, H.K.D.H. Bhadeshia, *Mater. Sci. Technol.* 8 (1992) 985–993. <http://dx.doi.org/10.1179/mst.1992.8.11.985>.
- [20] H.K.D.H. Bhadeshia, J.W. Christian, *Metall. Trans. A*. 21 (1990) 767–797. <http://dx.doi.org/10.1007/BF02656561>.
- [21] D. San Martin, K. Aarts, P. Rivera-Diaz-del-Castillo, N. van Dijk, E. Brück, S. van der Zwaag, *J. Magn. Magn. Mater.* 320 (2008) 1722–1728. <http://dx.doi.org/10.1016/j.jmmm.2008.02.002>.
- [22] M. Herbig, D. Raabe, Y.J. Li, P. Choi, S. Zaeferrer, S. Goto, *Phys. Rev. Lett.* 112 (2014) 126103. <http://dx.doi.org/10.1103/PhysRevLett.112.126103>.
- [23] Y. Li, D. Ponge, P. Choi, D. Raabe, *Ultramicroscopy* 159, Part 2 (2015) 240–247. 1st International Conference on Atom Probe Tomography & Microscopy.
- [24] S. Singh, in: E. Pereloma, D.V. Edmonds (Eds.), *Phase Transformations in Steels*, *Woodhead Publishing Series in Metals and Surface Engineering*, vol. 1, Woodhead Publishing. 2012, pp. 385–416. <http://dx.doi.org/10.1533/9780857096104.3.385>.
- [25] E. Swallow, H.K.D.H. Bhadeshia, *Mater. Sci. Technol.* 12 (1996) 121–125. <http://dx.doi.org/10.1179/mst.1996.12.2.121>.